Influences of crustal thickening in the Tibetan Plateau on loading modeling and inversion associated with water storage variation

CrossMark

Wang Hansheng[a,*], Xiang Longwei[a,b], Wu Patrick[c], Jia Lulu[d],
Jiang Liming[a], Shen Qiang[a], Steffen Holger[e]

[a] State Key Laboratory of Geodesy and Earth's Dynamics, Institute of Geodesy and Geophysics, Chinese Academy of Sciences, Wuhan 430077, China
[b] University of Chinese Academy of Sciences, Beijing 100049, China
[c] Department of Earth Sciences, University of Hong Kong, Hong Kong, China
[d] National Earthquake Infrastructure Service, Beijing 100036, China
[e] Lantmäteriet, 80182 Gävle, Sweden

ARTICLE INFO

ABSTRACT

We use the average crustal structure of the CRUST1.0 model for the Tibetan Plateau to establish a realistic earth model termed as TC1P, and data from the Global Land Data Assimilation System (GLDAS) hydrology model and Gravity Recovery and Climate Experiment (GRACE) data, to generate the hydrology signals assumed in this study. Modeling of surface radial displacements and gravity variation is performed using both TC1P and the global Preliminary Reference Earth Model (PREM). Furthermore, inversions of the hydrology signals based on simulated Global Positioning System (GPS) and GRACE data are performed using PREM. Results show that crust in TC1P is harder and softer than that in PREM above and below a depth of 15 km, respectively, causing larger differences in the computed load Love numbers and loading Green's functions. When annual hydrology signals are assumed, the differences of the radial displacements are found to be as large as approximately 0.6 mm for the truncated degree of 180; while for hydrology-trend signals the differences are very small. When annual hydrology signals and the trends are assumed, the differences in the surface gravity variation are very small. It is considered that TC1P can be used to efficiently remove the hydrological effects on the monitoring of crustal movement. It was also found that when PREM is used inappropriately, the inversion of the hydrology signals from simulated annual GPS signals can only recover approximately 88.0% of the annual hydrology signals for the truncated degree of 180, and the inversion of hydrology signals from the simulated trend GPS signals can recover approximately 92.5% for the truncated degree of 90. However, when using the simulated GRACE data, it is possible to recover almost 100%. Therefore, in future, the TC1P model can be used in the inversions of

ELSEVIER | **Production and Hosting by Elsevier on behalf of KeAi**

1.   Introduction

A new interdisciplinary research field that combines hydrology and geodesy (referred to here as hydro-geodesy) is emerging because of the innovative application of spaceborne gravimetry and Global Positioning System (GPS) techniques to enable the monitoring of near-surface water storage variation and their trends [1,2]. This new approach has considerable advantages over that of the more traditional approach, which uses micro-wave remote sensing, because it enables continuous measurements for the total amounts of regional or global water storage variations on both the Earth's surface and in deeper aquifers. Furthermore, the measurements can be performed in all weather conditions.

Hydro-geodesy measures the hydrology signals via inversion using observed gravity variation and surface radial displacements, with the assumption that the Earth's structure and material properties are well known [1,3]. It is therefore possible that use of an inappropriate earth model or the selection of inappropriate parameters could cause a bias in the inverted hydrology signals [4].

According to a newly released crustal model (CRUST1.0) [5], the Tibetan Plateau has an average crustal thickness of 65 km, and a maximum thickness of 80 km. Furthermore, the laterally averaged densities and P-wave and S-wave velocities within the top 65 km greatly deviate from those in the commonly used Preliminary Reference Earth Model (PREM) [6] (Fig. 1). It is therefore considered necessary to investigate the effects of earth model parameters on the estimated hydrology signals on the Tibetan Plateau [4].

Wang et al. [4] investigated the effects of crustal differences on the inversion of water trend rates on the Tibetan Plateau using the simulated Gravity Recovery And Climate Experiment (GRACE) and GPS data. They found that the effects of crustal differences on the inversion of hydrological trends were negligible when using simulated GRACE data, but were very prominent when using simulated GPS data. Note that the assumed hydrological trends were derived from the WaterGAP Global Hydrology Model (WGHM) [7], which considered major hydrological processes occurring between August 2002 and March 2011. However, it is now doubtful that the WGHM could reflect long term trends of water storage variation because unlike in North America and Scandinavia [1], surface hydrology observations are sparsely distributed in the Tibetan Plateau. For example, the WGHM interpreted larger trends of water level rises in the west and central Himalayan Mountain range, which may not be accurate [4]. Therefore, the Global Land Data Assimilation System (GLDAS) model [8] is used in this study, even though it does not include groundwater [1]. Jia et al. [9] investigated how radial displacements that are induced by the hydrological trends inverted from GRACE data (from 2003 to 2012), may be affected when using CRUST2.0 [10] instead of PREM to describe the average crustal structure in mainland China, with differences as large as 4% in mainland China, and 10% in the Tibetan Plateau.

In this study, we implement an extensive investigation with the aim of first gaining an understanding of the sensitivity of GPS-inferred surface radial displacements and surface gravity variation from terrestrial gravimetry on crustal structures. It is considered that this knowledge could then be used to correct for hydrology effects in the observed crustal movement and gravity variation [11,12]. And we describe the differences between the two selected earth models, TC1P and PREM; analyse the loading effects derived from the two earth models. Also, the effects of the earth model selection on the inversion of hydrology signals are presented. We aim to discern to what extent the crustal structure impacts the inversion of hydrologic signals as seen by the GLDAS hydrology model [8], and also the hydrological trend seen by GRACE.

2.   Earth models and assumed hydrology signals

In this section, we compare the parameters of the two earth models used, their load Love numbers (through which
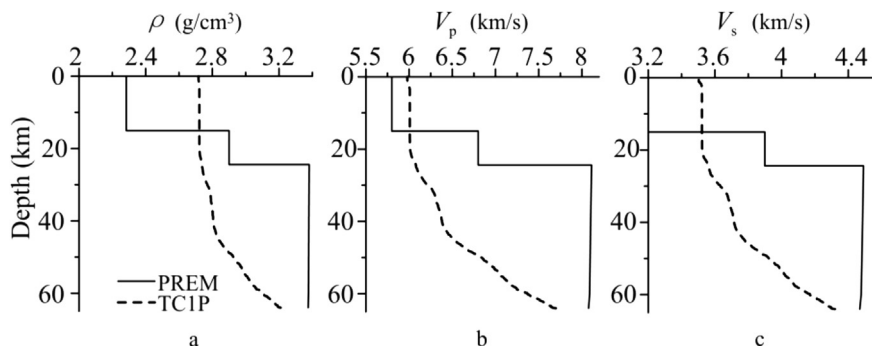

Fig. 1 − Comparisons of density and velocity profiles from surface to a depth of 65 km between the realistic TC1P model for the Tibetan Plateau and the global model PREM. ρ is density, and V_p and V_s are P-wave and S-wave velocities.

the hydrological signals are inverted), and their loading Green's functions (by which the surface displacements and gravity variation can be simulated). Finally, we show how the assumed hydrology signals are obtained.

2.1.   *Earth models*

We use two earth models: TC1P and PREM. TC1P is considered to be a realistic model, and it includes the thickened crust on the Tibetan Plateau as determined in CRUST1.0. Since the crust in the area has an average thickness of 65 km thick, the TC1P model uses the lateral averages of densities, V_p and V_s, given by CRUST1.0 within the top 65 km of crust, while the layered structure and parameters below a depth of 65 km are given by PREM. The three parameters of these two models are compared in Fig. 1. For the upper-most 15 km, the three parameters of TC1P are all larger than those given by PREM, but below a depth of 15 km they are significantly smaller than those of PREM. These pronounced differences could therefore have an adverse effect on the results of loading and the inversions of hydrology signals from geodetic data.

2.2.   *Load Love numbers and loading Green's functions*

Following Farrell [13], the degree n load Love numbers h_n, l_n, and k_n are related to radial and tangential displacements, and the potential perturbation respectively. The loading Green's functions for surface radial displacement (u_r), tangential displacement (v), and surface gravity change (g') are then computed, and the numerical method used for their computation is described in Wang et al. [14,15]. It is noted that our transformation method is used for the load Love numbers to improve the numerical stability at higher degrees.

The three load Love numbers for degrees 1−45000, and the three loading Green's functions are shown in Figs. 2 and 3. Fig 2 shows that the magnitudes of the three load Love numbers for TC1P are larger than those in the PREM for degree ranges 30−500, 40−1000, and 90−900 respectively, but are smaller for degrees over 1000. Similarly, Fig. 3 shows that the magnitudes for the three loading Green's functions in TC1P are also larger than those in PREM for angular distances (in degrees) of 0.008−0.4, 0.1−1.0, and 0.08−1.0 respectively, but are smaller for nearer angular distances. These discrepancies are caused by the relatively "soft" and "hard" crust in TC1P below and above a depth of 15 km.

2.3.   *Assumed hydrology signals*

Although the hydrology signals inverted from both GRACE data and given by the GLDAS model are crude approximations of the true hydrology signal in the study area, in this study we employ the "assumed hydrology signals," which are defined and computed as follows. Firstly, we use monthly GRACE data to derive the annual hydrology signals and their trends. Furthermore, we use monthly GLDAS hydrology data to derive the high resolution annual hydrology signals using the least square fitting technique. The annual hydrology signals and their trends, which are denoted by the equivalent water thickness (EWT) and EWT per year, respectively, are given by the surface mass density $\sigma(\theta, \phi)$ divided by the water density. The $\sigma(\theta, \phi)$ is decomposed into harmonics using:
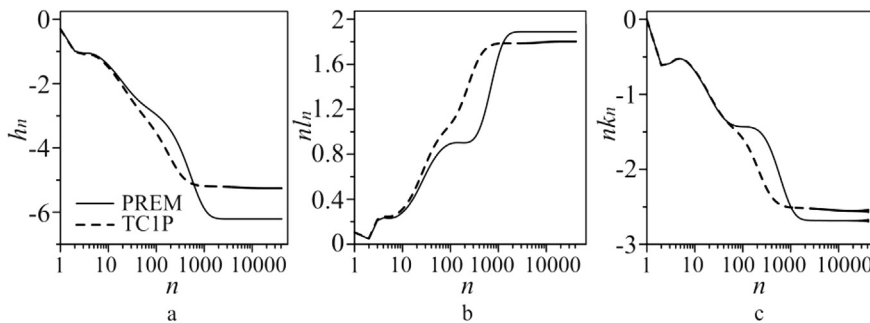

Fig. 2 − Comparison of load Love numbers between the TC1P and PREM models. h_n, l_n, and k_n represent the degree n load Love numbers for radial and tangential displacements, and potential perturbation respectively.
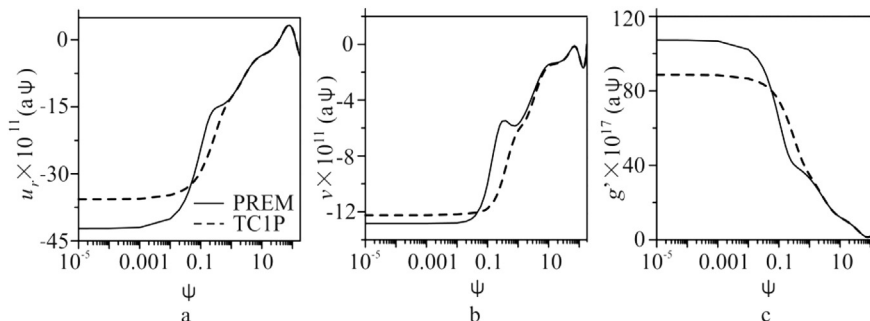

Fig. 3 − Comparison of Green's functions between TC1P and PREM models. u_r, v and g' (in cm, cm and cm/s² respectively) are the Green's functions for surface radial and tangential displacements, and surface gravity variation respectively. a is the Earth's radius (in cm), Ψ is the angular distance (in arc) between the observer and the point mass of 1 g.

$$\sigma(\theta,\phi) = \sum_{l=0}^{M}\sum_{m=0}^{l}(c_{lm}\cos m\phi + s_{lm}\sin m\phi)\tilde{P}_{lm}(\cos\theta) \quad (1)$$

where, θ and ϕ are co-latitude and longitude for regular grid points, $\tilde{P}_{lm}$ is the normalized associated Legendre polynomial, M is the truncated degree, and the coefficients are computed by [16]:

$$\begin{cases} c_{lm} = \dfrac{1}{4\pi}\int_{\Omega}\sigma(\theta',\varphi')\tilde{P}_{lm}(\cos\theta')\cos m\varphi'\,\mathrm{d}\Omega' \\ s_{lm} = \dfrac{1}{4\pi}\int_{\Omega}\sigma(\theta',\varphi')\tilde{P}_{lm}(\cos\theta')\sin m\varphi'\,\mathrm{d}\Omega' \end{cases} \quad (2)$$

where Ω denotes the integrated area with eastern longitudes of 65°−115° and northern latitudes of 15°−55°, and the gridded hydrology signals are given at regular grids, $\mathrm{d}\Omega' = \sin\theta'\mathrm{d}\theta'\mathrm{d}\varphi'$. Performing synthesis, as in equation (1), delivers the assumed hydrology signals used in this study at different truncated degrees.

In this study, GRACE data from January 2003 to October 2014 have a resolution of up to degree of 90, and GLDAS data from August 2002 to July 2007 have a spatial resolution of $1.0° \times 1.0°$ grids. The annual hydrology signals and their trends can be inverted from GRACE data for $M = 60$ and 90, and the annual hydrology signals are given by GLDAS data for $M = 180$. The inversion method used for hydrology signals employing GRACE data can be found in Wahr et al. [3]. Furthermore, the load Love numbers used are those shown in Fig. 2, with reference to the TC1P model. For simplicity, we use the amplitudes of the assumed annual hydrology signals to express the signals themselves, and we neglect the differences of the phases for different grid points.

Fig. 4a−c show the annual hydrology signals for $M = 60$, 90, and 180, and Fig. 4d, e show the trends of the hydrology signals for $M = 60$ and 90. To check the reliability of the assumed

a-Annual hydro.,degree 60

b-Annual hydro.,degree 90

c-Annual hydro.,degree 180

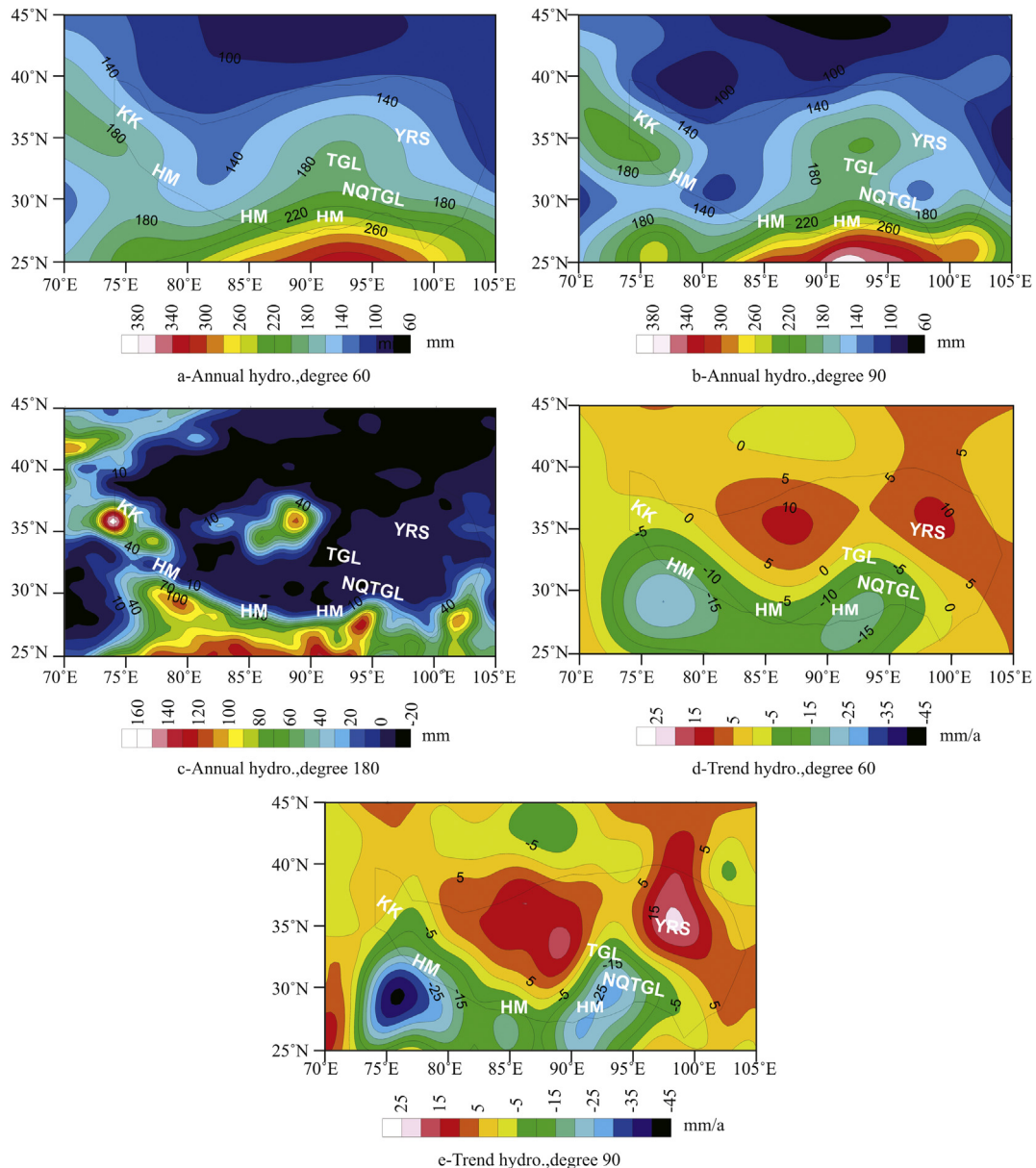d-Trend hydro.,degree 60

e-Trend hydro.,degree 90

Fig. 4 − The assumed hydrology signals derived from the GLDAS hydrology model c, and inverted from GRACE data a, b, d and e. a, b and c are the annual signals for $M = 60$, 90, and 180, respectively; d and e are the trend signals for $M = 60$ and 90. KK, HM, NQTGL, TGL, and YRS are abbreviations for the Karakorum, Himalaya, Nyaiqentanglha, Tanggula, and Yellow River sources, respectively.

hydrology signals, a comparison was made with precipitation data [17], and a rough agreement was found between the distribution of primary hydrology anomalies in the Tibetan Plateau and its surroundings (the comparisons are not shown here). However, for the same spatial resolutions (e.g., corresponding to $M = 90$), the magnitudes of the annual hydrology signals from GLDAS were found to be far less than those from GRACE. This was considered to be possibly due to the fact that GLDAS does not include the water storage changes in deeper aquifers, and that the sporadic ground observations employed may also cause larger uncertainties for the model.

In the next section, to make comparisons between GRACE and GLDAS for the assumed annual hydrology signals and loading effects, it is necessary to enlarge the results for GLDAS empirically by a factor of 2.5 (which is found for $M = 90$).

In Fig. 4a, b, the larger annual hydrology signals for $M = 60$ and 90 are found in the central plateau, with magnitudes of approximately 260 mm, showing an increasing magnitude from the north to south. Regional signals are found to the south of Karakorum and around Tanggula, with magnitudes of 180 mm. This shows that when a higher truncated degree is used, the regional signals become more pronounced. This is particularly true in Fig. 4c, where $M = 180$. The hydrology signals to the south of Karakorum and north of the plateau have magnitudes of approximately 400 and 275 mm, respectively. It is also of note that the annual hydrology signals are very small for most parts of the plateau for $M = 180$, and that the obvious signals found in the south for $M = 60$ and 90 may be caused by the leakage of the large signals from outside. Fig. 4d, e show the assumed hydrology trend signals for $M = 60$ and 90. The larger water trend appears in the center of the plateau and in the Yellow River source region. For the two regions, the magnitudes are approximately 10 and 10 mm/a for $M = 60$, and approximately 15 and 20 mm/a for $M = 90$. Furthermore, larger trend decreases are found because of the ice melting in the regions of the Karakorum, Himalaya, and Nyaiqentanglha Mountains, with magnitudes of approximately 15 and 25 mm/a for the two truncated degrees, respectively. However, for the annual hydrology signals, the trend signals are also impacted partly by the leakage of strong signals from outside.

The assumed hydrology signals shown above can be used to investigate the effects of earth model parameters on the loading effects and on the inversions of hydrology signals with different spatial resolutions, based on the simulated GPS and GRACE data, respectively.

3. Loading effects associated with hydrology signals

For both the realistic earth model TC1P and the traditionally used earth model PREM, the surface radial displacements and surface gravity variation induced by the assumed hydrology signals can be respectively computed by

$$u_r(\theta,\phi) = \frac{3}{\bar{\rho}} \sum_{l=0}^{M} \frac{h_l}{2l+1} \sum_{m=0}^{l} (c_{lm} \cos m\phi + s_{lm} \sin m\varphi)\tilde{P}_{lm}(\cos\theta) \quad (3)$$

and

$$\delta g'(\theta,\varphi) = 4\pi G \sum_{l=0}^{M} \frac{(l+1)(1+k_l) - 2h_l}{2l+1} \sum_{m=0}^{l} (c_{lm} \cos m\varphi + s_{lm} \sin m\varphi)\tilde{P}_{lm}(\cos\theta) \quad (4)$$

where, h_l and k_l are the load Love numbers for radial displacement and potential perturbation based on the two earth models, as shown in Fig. 2; $\bar{\rho}$ is the average density of the Earth and G is the Newtonian gravitational constant.

Fig. 5a, c, e show the predicted radial displacements of the TC1P model induced by the assumed annual hydrology signals for $M = 60$, 90, and 180, respectively; and Fig. 6 a, c show those induced by the assumed hydrology trend signals for $M = 60$ and 90. It can be seen that the patterns of the radial displacements are very similar to those of the corresponding assumed hydrology signals, as in Fig. 4a−c and in Fig. 4d, e. However, they become smoother than the assumed hydrology signals, due to the low-pass filtering of the elastic lithosphere. The negative (positive) results indicate that the crust subsides (rebounds) due to the adding (removing) of the water mass. These magnitudes are of approximately 17, 18, and 9.0 mm (magnified by a factor of 2.5) in Fig. 5a, c, e, and approximately 0.4 and 0.6 mm/a in Fig. 6a, c, implying that the annual and trend hydrology signals can be measured by continuous GPS. In Fig. 5b, d, f and in Fig. 6b, d, the differences using the values predicted from PREM are found to become larger as the truncated degree is increased. When the annual hydrology signals are assumed, the magnitudes are approximately 0.40, 0.45, and 0.60 mm for $M = 60$, 90, and 180, respectively, and when the trend hydrology signals are assumed they are approximately 0.03 and 0.04 mm/a for $M = 60$ and 90, respectively. However, such differences in the radial displacements between two earth models are identified in annual GPS signals but not in GPS trend signals.

There are similar characteristics in the patterns of the predicted surface gravity variation for TC1P, and the differences with those from PREM in Figs. 7 and 8, as the gravity variation mainly reflect the radial displacements. Fig. 7a, c, e show the annual gravity variation with magnitudes of approximately 15, 15, and 21 μGal for $M = 60$, 90, and 180, respectively; and Fig. 8a, c show magnitudes of 0.8 μGal, 1.2 μGal for the trend gravity variation. These values show that the annual hydrology signals can be captured by surface repeating gravimetry, but that the trend hydrology signals are difficult to measure for $M = 60$ and 90. The corresponding differences with those from PREM are shown in Fig. 7b, d, f and in Fig. 8b, d, with magnitudes of approximately 0.15 μGal, 0.15 μGal, 0.2 μGal, 0.08 μGal/a and 0.14 μGal/a, respectively. This implies that it is difficult to identify any differences in the gravity variation between the two earth models in relation to the annual and trend gravity signals observed from ground gravimetry.

4. Simulated inversions for hydrology signals

4.1. Inversion formulas

As stated above, the assumed hydrology signals are derived from GRACE data and GLDAS, and these can be further
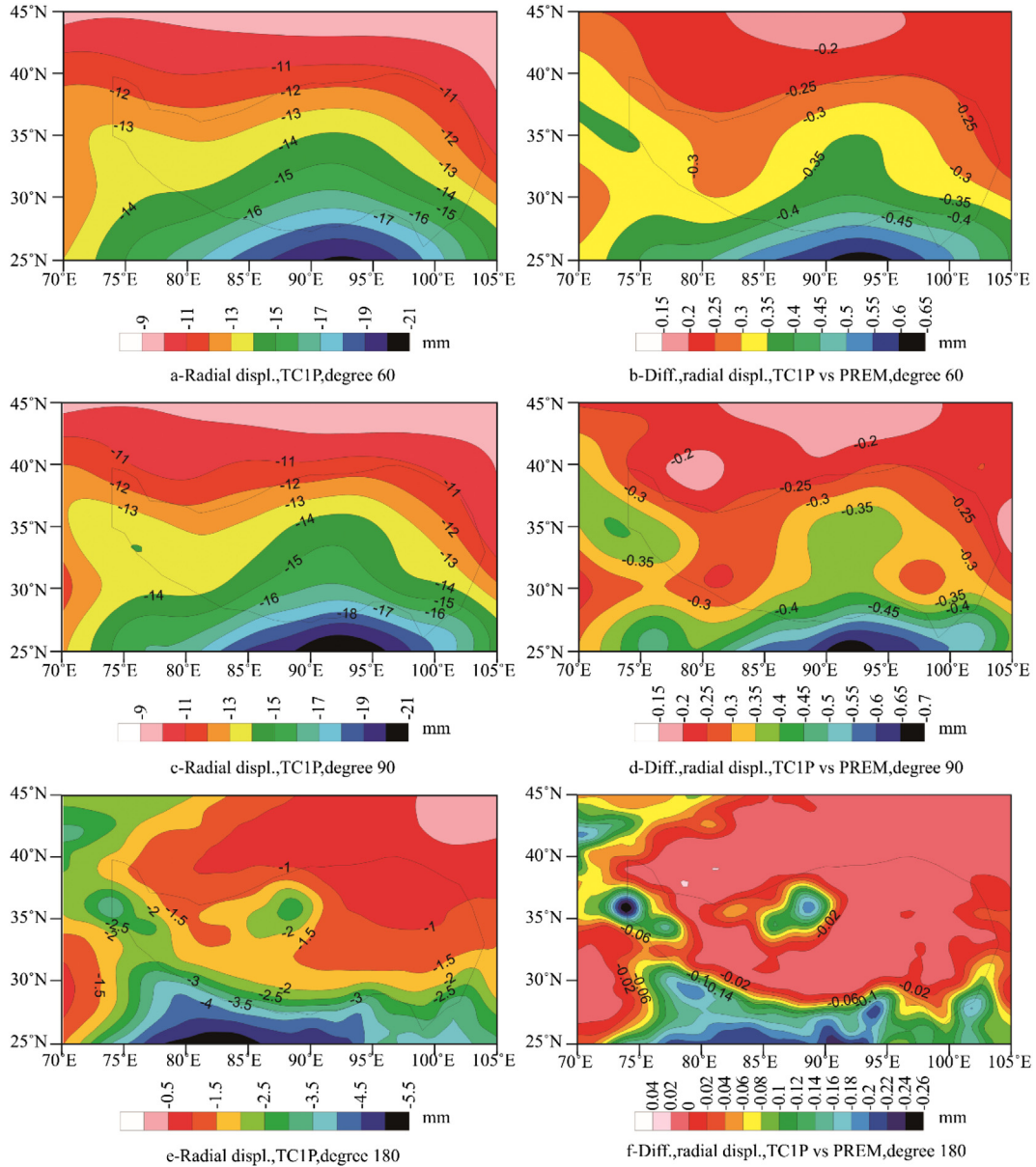
Fig. 5 − Radial displacements (a, c, e) from the TC1P model induced by the assumed annual hydrology signals; and the differences (b, d, f) from the model PREM. a and b, c and d, and e and f are for M = 60, 90, and 180, respectively. The polygon denotes the Tibetan Plateau.

used to simulate GRACE gravity variation and GPS radial displacements using the load Love numbers (h_l,k_l) of the realistic model TC1P. When implementing the inversions of hydrology signals (by the area density of EWT changes or EWT per year) from the simulated GPS and GRACE data, it is likely that using the load Love numbers (h'_l, k'_l) based on PREM will lead to errors. Therefore, Wang et al. [4] deduced the following formulas for the inversions:

$$\sigma^{GRACE}(\theta, \varphi) = \sum_{l=0}^{M} \sum_{m=0}^{l} \frac{1+k_l}{1+k'_l}(c_{lm} \cos m\varphi + s_{lm} \sin m\varphi)\tilde{P}_{lm}(\cos \theta)$$

(5)

$$\sigma^{GPS}(\theta, \varphi) = \sum_{l=0}^{M} \sum_{m=0}^{l} \frac{h_l}{h'_l}(c_{lm} \cos m\varphi + s_{lm} \sin m\varphi)\tilde{P}(\cos \theta)$$

(6)

Consequently, in addition to the load Love numbers for the two earth models, the harmonic coefficients of the assumed hydrology signals, given by equation (2), are required in order to finish the simulated inversions using simulated GPS and GRACE data, respectively (the simulated GPS and GRACE data are not shown here).
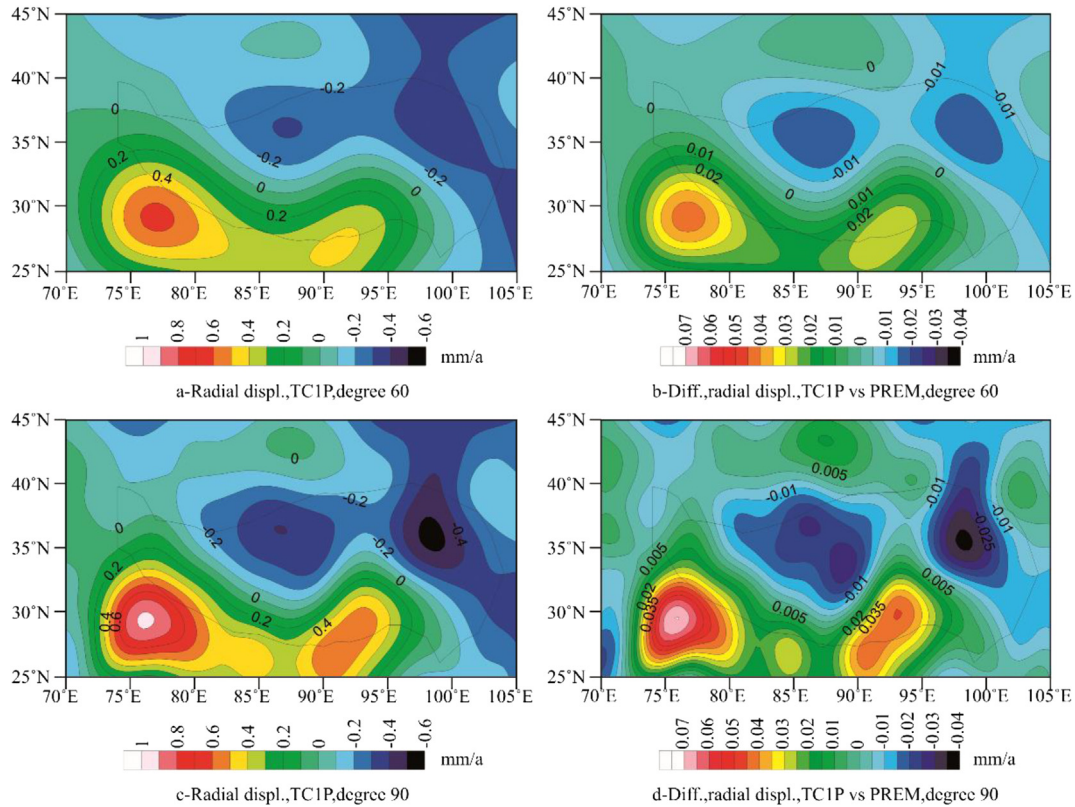
Fig. 6 − Radial displacements (a, c) from the TC1P model induced by the assumed trend hydrology signals; and the differences (b, d) using model PREM. a and b, c and d are for M = 60, 90, respectively.

4.2.   *Inversion results*

When PREM is used for inversions of the hydrology signals from simulated GPS and GRACE data using equations (5) and (6), errors may occur in relation to the inversions. Fig. 9 c, d, and Fig. 10 b show the differences between the annual hydrology signals inverted from the simulated GPS data and the assumed hydrology signals (Fig. 9a, b and Fig. 10a) for M = 60, 90, and 180, respectively. The magnitudes are approximately 7 mm, 8 mm, and 50 mm, which accounts for approximately 2.8%, 3.1%, and 12.0% of the assumed hydrology signals. Similarly, Fig. 9e, f, and Fig. 10c show the differences using the simulated GRACE data, which are found to be very small, with magnitudes of 0.08, 0.1, and 0.4 mm.

Fig. 11 c, d show the differences between the hydrology trend signals inverted from the simulated GPS data, and the assumed hydrology signals (Fig. 11a, b) for M = 60 and 90. The magnitudes are approximately 0.5 and 1.5 mm/a, accounting for approximately 5.0% and 7.5% of the assumed hydrology signals. Similarly, Fig. 11e, f show the differences using simulated GRACE data for M = 60 and 90, which are also found to be very small and have magnitudes of approximately 0.014 and 0.018 mm/a, respectively.

As shown above, the inversions based on the simulated GRACE data are far more capable of retrieving the assumed annual and trend hydrology signals than when based on the GPS data. The reason for this is that GRACE signals are dominated by contributions from the Newtonian attractions of the hydrology signals, and are less sensitive to the mass redistribution of the solid earth due to loading deformation.

5.   Conclusions

In this study, we used hydrology models with different resolutions for the Tibetan Plateau and its surroundings, and the realistic TC1P model, which has an average crustal structure of the plateau that is derived from the newly released 1° × 1° CRUST1.0 model, to carefully investigate the loading effects on the load Love numbers and the loading Green's functions, such as surface radial displacements and gravity variation induced by assumed hydrology signals. We also investigated the effects of the global model PREM on the inversion of hydrology signals based on simulated GPS and GRACE data. Our findings are summarized in the points below.

First, we find that the crust for TC1P is harder than PREM above a depth of 15 km, but softer below this depth. This causes the load Love numbers for the TC1P model to have larger magnitudes for degrees between tens and hundreds, but smaller magnitudes for degrees over 1000. In this respect, the three loading Green's functions have larger amplitudes within 10−100 km, but become smaller within 10 km.
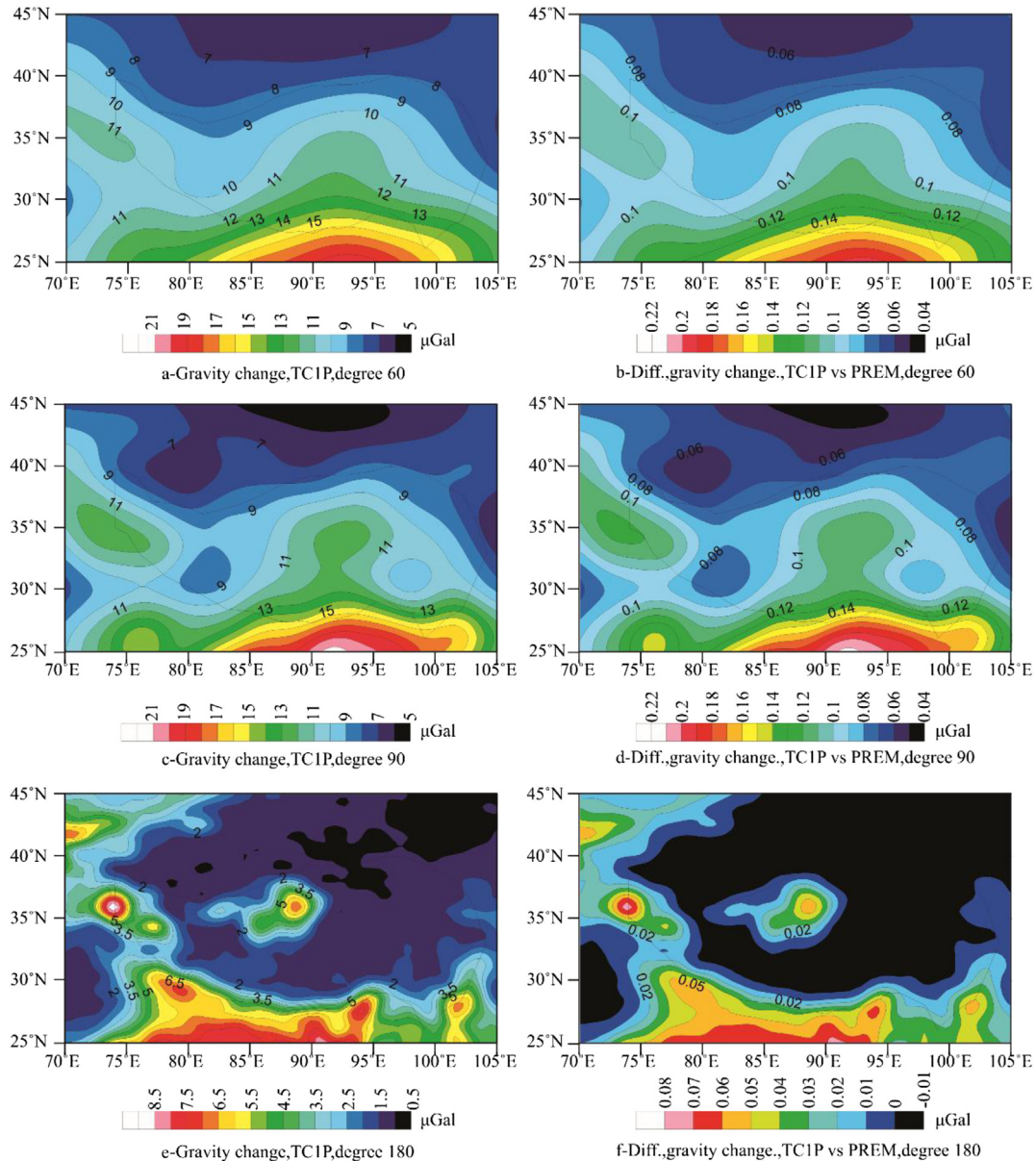
Fig. 7 − **Similar to Fig. 5, except for surface gravity variation.**

It was also found that the differences for radial displacements and gravity variation predicted by the two models increase in line with an increase in the truncated degree. For annual radial displacements, the differences have magnitudes of approximately 0.40, 0.45, and 0.60 mm for truncated degrees of 60, 90 and 180 respectively, and these effects could be readily observed. However, the differences in the trends of radial displacements are too small to be identified. For annual surface gravity variation, the differences have magnitudes of approximately 0.15, 0.15, and 0.2 µGal for three truncated degrees, and the magnitude of differences for the trend in surface gravity variation are approximately 0.08 and 0.14 µGal/a for truncated degrees of 60 and 90; such values are hard to identify using ground gravity measurements.

Furthermore, we discovered that due to the inappropriate use of PREM, the inversions of hydrology signals from simulated annual GPS data can only recover approximately 97.2%, 96.9%, and 88.0% of the assumed annual hydrology signals for truncated degrees of 60, 90 and 180; and that the inversion of hydrology signals from simulated trend GPS data can only recover 95.0% and 92.5% of the assumed trend hydrology signals for the truncated degrees of 60 and 90, respectively. However, the inversion of hydrology signals from the simulated GRACE data can recover almost 100% of the assumed hydrology signals.

It is therefore considered, that TC1P can be used for the inversion of hydrology signals based on GPS network data in the future. However, PREM is also valid for inversions from GRACE data with resolutions of approximately 220 km or larger. We suggest the use of the TC1P model for the Tibetan Plateau because this would help to efficiently remove the hydrological effects in relation to the monitoring of crustal
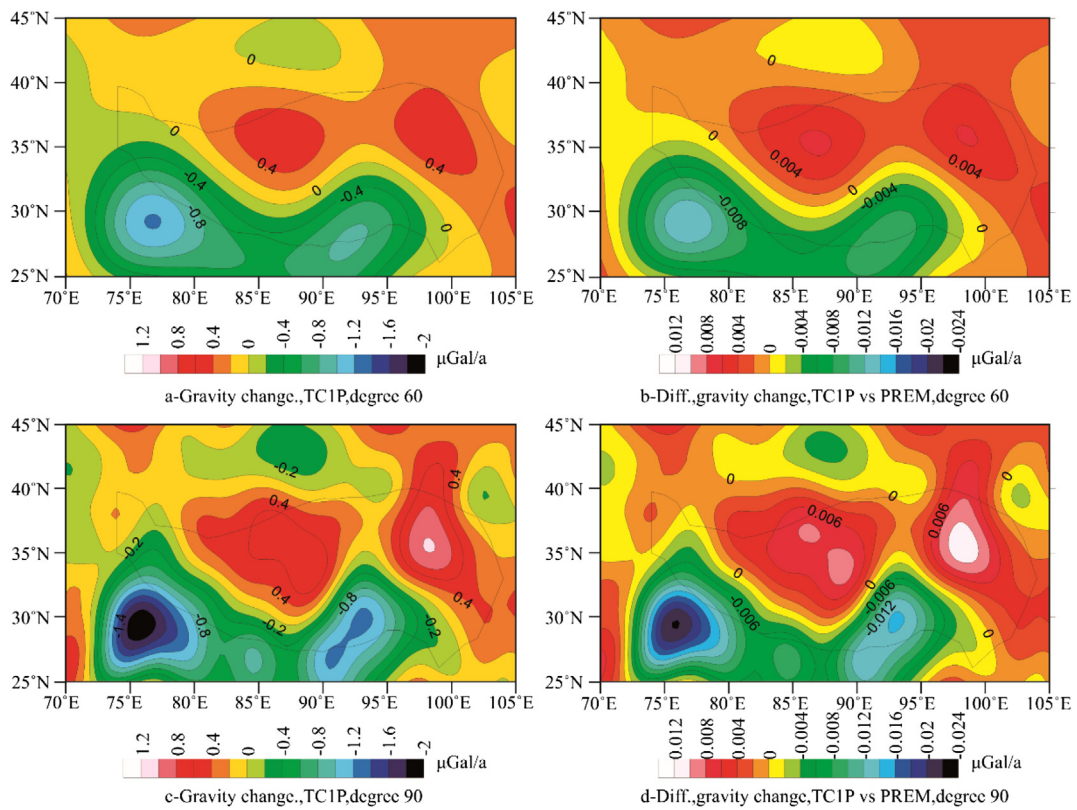
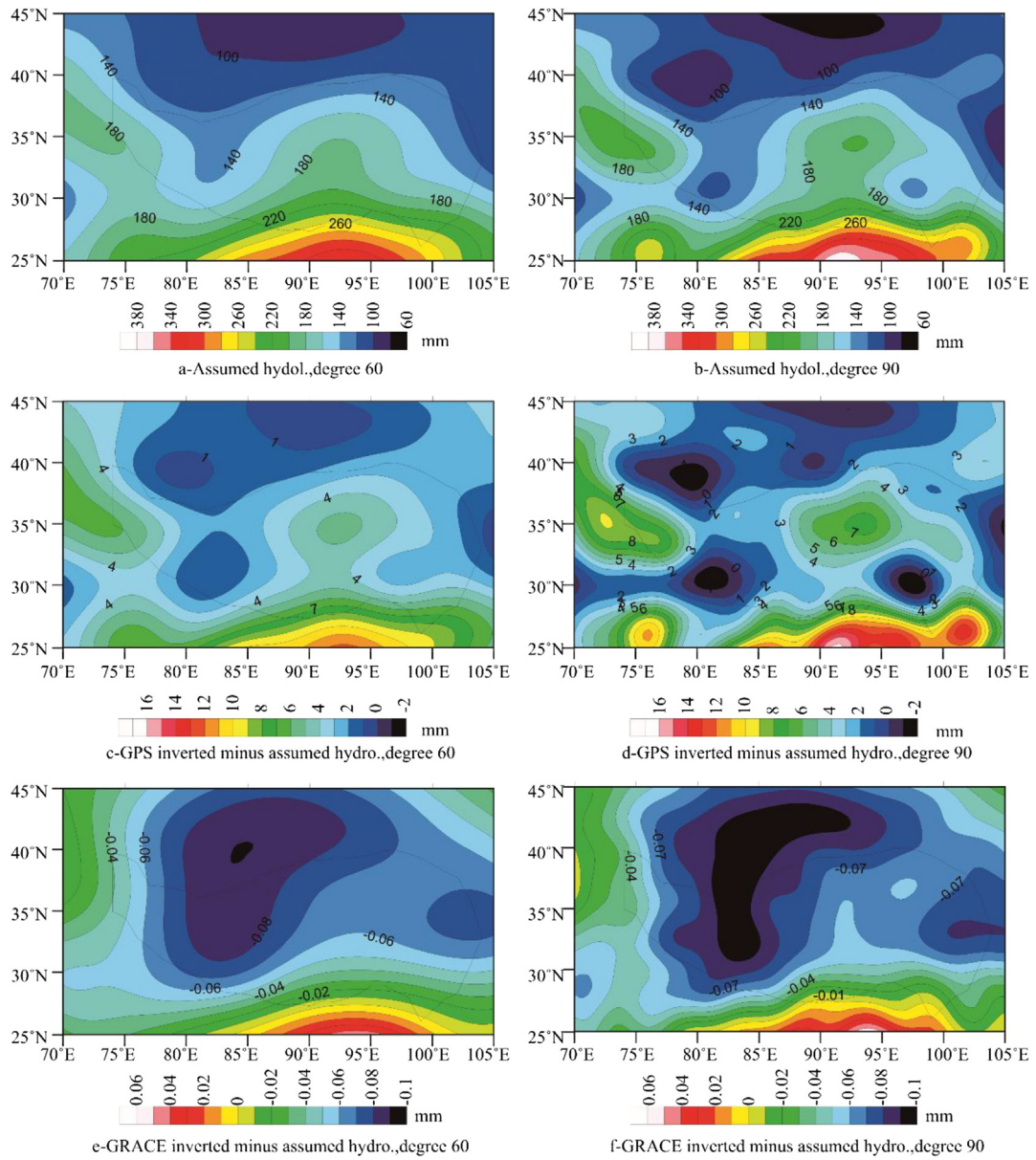Fig. 8 − Similar to Fig. 6, except for surface gravity variation.

Fig. 9 − Differences between the annual hydrology signals inverted from the simulated data based on TC1P model, and the assumed signals. a The assumed annual signals derived from GRACE data for M = 60; c differences when using the simulated GPS data for M = 60, and e differences when using the simulated GRACE data for M = 60. b, d, and f are similar to a, c, and e, respectively, but for M = 90.
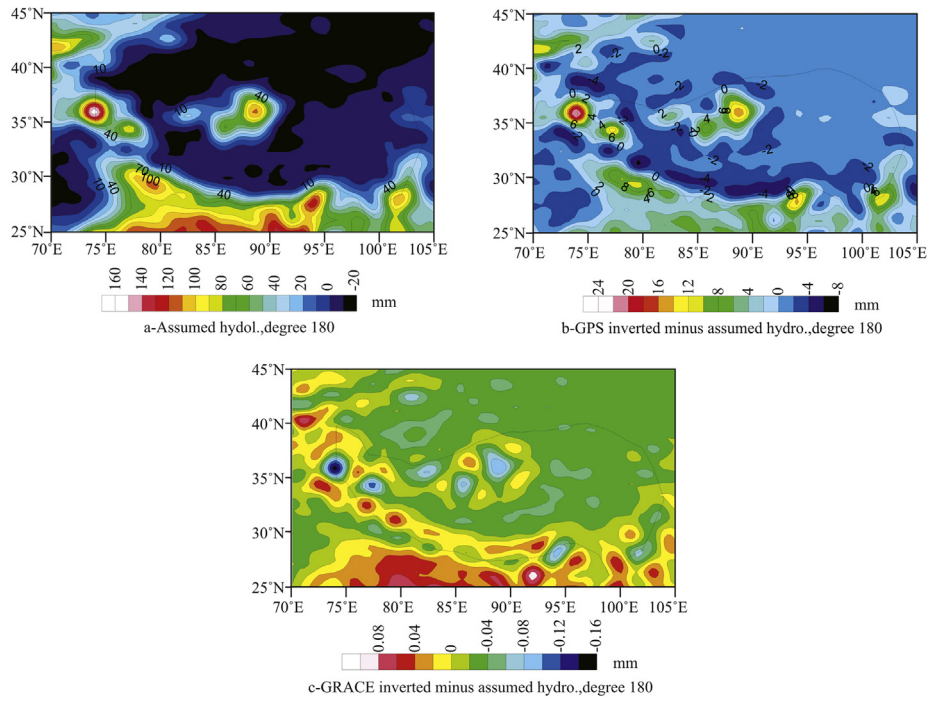
Fig. 10 — Similar to Fig. 9, except for the truncated degree of 180. The assumed annual hydrology signals are derived from GLDAS.
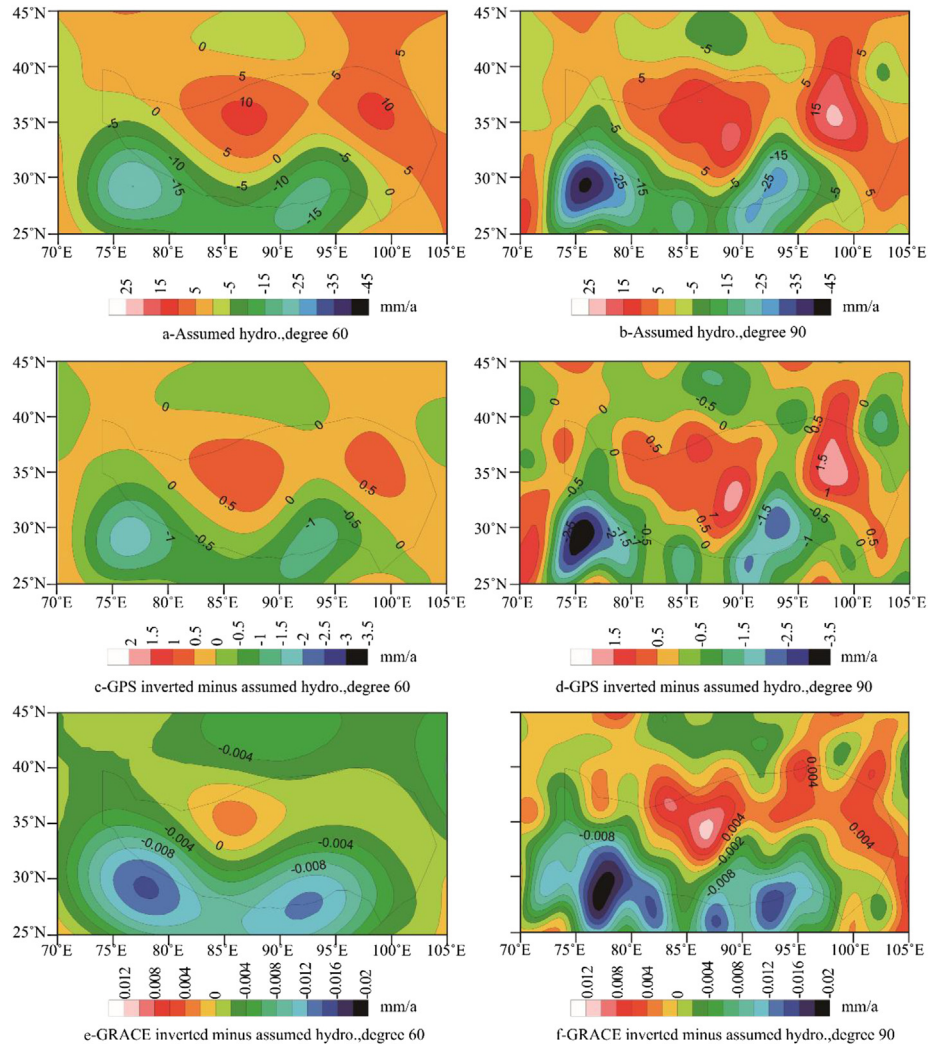

Fig. 11 — Similar to Fig. 9, except for the assumed trend hydrology signals. The assumed trend hydrology signals are derived from GRACE data.

movements and also enable the better recover of hydrology signals from GPS and GRACE data. The load Love numbers and the loading Green's functions are available for all academic communities.

Acknowledgement

REFERENCES

[1] Wang H, Jia L, Steffen H, Wu P, Jiang L, Hsu H, et al. Increased water storage in North America and Scandinavia from GRACE gravity data. Nat Geosci 2013;6(1):38—42.

[2] Wang Hansheng, Wang Zhiyong, Yuan Xudong, Wu Patrick, Rangelova Elena. Water storage changes in Three Gorges water systems area inferred from GRACE time-variable gravity data. Chinese J Geophys 2007;50(3):730—6 [in Chinese].

[3] Wahr J, Molenaar M, Bryan F. Time variability of the Earth's gravity field: hydrological and oceanic effects and their possible detection using GRACE. J Geophys Res 1998;103(B12):30205—29.

[4] Wang H, Xiang L, Wu P, Steffen H, Jia L, Jiang L, et al. Effects of the Tibetan Plateau crustal structure on the inversion of water trend rates using simulated GRACE/GPS data. Terr Atmos Ocean Sci 2013;24(41):505—12.

[5] Laske G, Masters G, Ma Z, Pasyanos M. Update on CRUST1.0-A 1-degree global model of Earth's crust. Geophys Res Abstr 2013;15. Abstract EGU2013-2658.

[6] Dziewonski AM, Anderson DL. Preliminary reference Earth model. Phys Earth Planet Interiors 1981;25(4):297—356.

[7] Döll P, Kaspar F, Lehner B. A global hydrological model for deriving water availability indicators: model tuning and validation. J Hydrology 2003;270(1—2):105—34.

[8] Rodell M, Houser PR, Jambor U, Gottschalck J, Mitchell K, Meng C, et al. The Global Land Data Assimilation System. Bull Am Meteorological Soc 2004;85(3):381—94.

[9] Jia L, Xiang L, Wang H. Effects of crustal structure for estimation of vertical load deformation on the solid earth using GRACE in China mainland. Adv Earth Sci 2014;29(7):828—34.

[10] Bassin C, Laske G, Masters G. The current limits of resolution for surface wave tomography in North America. EOS Trans AGU 2000;81:F897.

[11] Wang H, Hsu H, Zhu Y. Prediction of surface horizontal displacements, and gravity and tilt changes caused by filling the Three Gorges Reservoir. J Geodesy 2002;76(2):105—14.

[12] Wang H. Surface vertical displacements and level plane changes in the front reservoir area caused by filling the Three Gorges Reservoir. J Geophys Res 2000;105(B6):13211—20.

[13] Farrell WE. Deformation of the Earth by surface loads. Rev Geophys Space Phys 1972;10(3):761—97.

[14] Wang Hansheng, Hsu Houze, Li Guoying. Improvement of computations of load Love numbers of SNREI earth model. Chin J Geophys 1996;39(suppl.):182—9 [in Chinese].

[15] Wang H, Xiang L, Jia L, Jiang L, Wang Z, Hu B, et al. Load Love numbers and Green's functions for elastic Earth models PREM, iasp91, ak135, and modified models with refined crustal structure from Crust 2.0. Comput Geosciences 2012;49:190—9.

[16] Wang H, Wu P, Wang Z. An approach for spherical harmonic analysis of non-smooth data. Comput Geosciences 2006;32:1654—68.

[17] Adler RF, Huffman GJ, Chang A, Ferraro R, Xie P, Janowiak J, et al. The version-2 global precipitation climatology project (GPCP) monthly precipitation analysis (1979—present). J Hydrometeorol 2002;4(6):1147—67.

Wang Hansheng is a professor at Institute of Geodesy and Geophysics, Chinese Academy of Sciences, China. His study interests include the loading theory and modeling method, last glacial isostatic adjustment (GIA) modeling and mantle rheology, the theory and method associated with elastic loading or GIA or both for monitoring water storage change using geodetic observations. They have proposed a transform approach to improve the numerical stability for higher degree load Love numbers, with which the load Love numbers extending to degree 45000 and the Green's functions are calculated and provided for global average earth model (PREM. Ak135, iasp91) and Tibetan Plateau model (TC1P). Taking into account the lateral heterogeneity in mantle viscosity and lithospheric thickness, they have established a GIA model (RF3L20beta = 0.4), which estimates the lateral variation of mantle viscosity, and predicts the radial and tangential crustal motions, gravity change, and absolute and relative sea level changes. In addition, they have developed a separation approach for extracting hydrology (or water storage change, ice melting etc) signal and GIA signal in last glaciated areas using GRACE together with GPS data, with which the decadal water increases are found in the Canadian Prairies and the Great Lakes area, and at the southern tip of the Scandinavian Peninsula.